CHEMICAL ENGINEERING TRANSACTIONS
VOL. 78, 2020
A publication of AIDIC
The Italian Association of Chemical Engineering
Online at www.cetjournal.it
Guest Editors: Jeng Shiun Lim, Nor Alafiza Yunus, Jiří Jaromír Klemeš

ISBN 978-88-95608-76-1; **ISSN** 2283-9216
DOI: 10.3303/CET2078060

Fabrication of TiO_2 Monolithic Photocatalyst and Evaluation of its Antibacterial Activity under Simulated Solar Irradiation

Diep N. Pham, Minh-Vien Le*, Hoang Anh Hoang, Xuan T.T. Tran, Tuan-Anh Nguyen

Faculty of Chemical Engineering, Ho Chi Minh City University of Technology, VNU-HCM, Ho Chi Minh City 700000, Vietnam
lmvien@hcmut.edu.vn

In this study, the TiO_2 nanoparticles were coated on the monolithic surface by a dip-coating technique. Characterization of synthesized samples was determined by X-ray diffraction. Antibacterial application of the samples was investigated under simulated solar irradiation on *Escherichia coli (E. coli)* bacteria. A 5.7 log CFU mL^{-1} decrease of *E. coli* was observed with TiO_2 nanoparticles after 3 h irradiation, whereas the number of surviving *E. coli* cells decreased by 2.7 log CFU mL^{-1} with monolithic TiO_2 at the same irradiating condition. Despite the reduction of photocatalytic antibacterial effect, the results confirmed the photocatalytic antibacterial activity of monolithic TiO_2 under simulated sunlight irradiation as well as revealed its potential in practical water treatment applications.

1. Introduction

The rapidly accelerating urbanization-industrialization process in the 21st Century has helped the economy of some countries develop notably. On the other hand, its parallel serious consequences are climate change as well as emerging issues such as degradation and pollution of environment (Liu and Bae, 2018). Water polluting agents includes harmful microorganisms, heavy metals, organic and inorganic chemicals (Zeliger, 2008). The harmful microorganisms cause really dangerous human infections and inflammations in blood, skin, eyes; gastrointestinal tract, brain, etc. (Baldursson and Karanis, 2011). The clean water shortage for over 2 billion people on the world leads to at least half a million deaths from diarrhoeal each year (Pichel et al., 2019). As a result, more difficulty in approaching clean water sources has received more concerns, especially in developing countries. That is why the topic of polluted water treatment, especially drinking water disinfection always is cared for and researched urgently.

Current water disinfection methods are limited in worldwide applications and scale-up due to some obstructions. For instance, disinfection using antiseptics (Hrudey, 2009) and ozonation (Yang et al., 2012) damages human health due to toxic by-product. Reverse osmosis and nano-filtration membranes remove not only whole microorganisms and contaminants but also minerals which are important essential for human health (Ismail et al., 2019). Disinfection using UV light (Lui et al., 2016) and a thermal treatment process (Feng et al., 2004) always requires high energy as well as accommodates re-infecting risks. Alternative methods have been developed constantly to overcome these obstructions. Photocatalysis techniques were applied for an advanced oxidation technology which disinfects with free radicals and reactive oxygen species (Lee and Park, 2013). The most important benefits of photocatalysts are operability at low concentration, reusability for a long time and non-existence of toxic by-products. If the photocatalysis is activated by solar light as a renewable source, it will obviously become a green solution in water treatment.

TiO_2 nanomaterial is known as a popular photocatalyst because of its efficiency in degradation of organic chemicals (Gaya and Abdullah, 2008) and antibacterial. In particular, the photocatalytic antibacterial activity of TiO_2 is effective on many types of microorganism such as algae, viruses, fungi, and bacteria (Laxma Reddy et al., 2017). A pure anatase TiO_2 nanomaterial with particle size of 5.3 nm shown its antibacterial activity noticeably after 12 h visible irradiation due to a 1 log CFU mL^{-1} decrease of *E. coli* (Cao et al., 2013). Another single-phase anatase TiO_2 prepared by a sol-gel method decreased by approximately 3.4 log CFU mL^{-1} of *E. coli* after 1 h UVC irradiation (Moongraksathum and Chen, 2018). As evidence, the commercial Degussa P25

Paper Received: 27/04/2019; Revised: 20/08/2019; Accepted: 31/10/2019
Please cite this article as: Pham D.N., Le M.-V., Hoang H.A., Tran X.T., Nguyen T.-A., 2020, Fabrication of TiO_2 Monolithic Photocatalyst and Evaluation of its Antibacterial Activity under Simulated Solar Irradiation, Chemical Engineering Transactions, 78, 355-360 DOI:10.3303/CET2078060

TiO_2 was confirmed to cause a 4 log CFU mL^{-1} reduction of *E. coli* after 1 h simulated solar irradiation (Gumy et al., 2006). In addition, TiO_2 nanomaterials also indicate more dominance, for example, non-toxicity(Nguyen et al., 2019), lower cost than other photo-catalysts (Makhdoomi et al., 2015), inert nature (Gaya and Abdullah, 2008) and high biological stability (Lee and Park, 2013). All the advantages show that TiO_2 is capable of disinfection treatment for drinking water.

In contrast, nano-size of TiO_2 cause limitation in practical applications on account of separating nanoparticles out of water and reuse. Reusing TiO_2 nanoparticles, which requires lots of complex recovery equipment, leads to high cost of antibacterial process. To improve TiO_2 reusability, TiO_2 nanopowders have been gradually replaced by nanosized TiO_2 coated on inert substrates. TiO_2 was deposited on cotton fiber to obtain cotton/TiO_2 composites which indicated antibacterial activity against *E. coli* bacteria under short UV irradiation after 5 washing cycles (Galkina et al., 2014). A sol-gel method combined with a dip-coating technique was used to fabricate TiO_2 thin films (Sasani Ghamsari and Bahramian, 2008). TiO_2 coated on glass was also prepared with the corresponding way (Hakki et al., 2018). These types of substrate are seemingly ill-suited to take a key role in drinking water treatment equipment. Another prefer substrate towards water treatment applications is a monolith. Ceramic monoliths are lighter than metallic monoliths and variable in size as well as morphology such as spherical, cubic or cylindrical shape. Cylindrical honeycomb monoliths with lots of channels on the inside lead to larger surface area (Heck et al., 2001) which enhances contacts between TiO_2 and bacteria. The purpose of this study is surveying influence factors to find a good condition for fabricating a photocatalytic-antibacterial material which is able to withdraw and reuse as well as evaluating initially antibacterial activity of this material.

In this study, single-phase anatase TiO_2 was coated on channel surface of honeycomb monoliths. The synthesized TiO_2 was characterized by using X-ray diffraction (XRD) and its photocatalytic antibacterial activity was evaluated on *E. coli* bacteria by spread plate method. Monolith photo-reactor design in this study was referred from a previous study in gas treatment application (Tahir, 2018). These results are initial investigation for monolithic TiO_2 application in further water treatment studies.

2. Experimental

2.1 Materials and reagents

All materials and reagents were used without purification. Titanium n-butoxide (TNB, 99%) as titania precursor was obtained from Across Organics. Tetraethyl orthosilicate (TEOS, 99 %) as a silicon source was purchased from Merck Chemical Company. Acetylacetone (AcAc, 99%), polyethylene glycol (PEG, MW = 20,000), sodium chloride (99%), poly peptone, bacto yeast extract, and agar were all supplied by Merck Chemical Company. Nitric acid (HNO_3, 65%) was purchased from Scharlab in Spain. Deionized water was used in all experiments. Commercial honeycomb monoliths (∅4 x 10 cm) including 177 channels per 2 mm x 2 mm were supplied by Chauger Honeycomb Ceramics Company in Taiwan.

2.2 Preparation of nano-material

2.2.1 Synthesis of TiO_2 nanopowders

TiO_2 nanopowders were synthesized according to a sol-gel method from solutions A and B as follow. EtOH, AcAc, and PEG were added sequentially to TNB with the TNB : EtOH : AcAc molar ratio of 1 : 10 : 1 and the PEG : TiO_2 weight ratio of 1 : 2, then this mixture was dissolved at 40 °C for 30 min to obtain the solution A. H_2O was added to EtOH with the H_2O : EtOH molar ratios of 2 : 10, 4 : 10 or 6 : 10 to obtain the solution B. pH value of the solution B was adjusted to 2 by using HNO_3. The solution B was added dropwise to the solution A for 2.5 h at room temperature. This mixture was heated at 80 °C for 2 h afterwards to get a TiO_2 solution. In the next step, the TiO_2 solution was dried at 120 °C for 2.5 h before calcination at 500 °C or 550 °C for 2 h with a heating rate of 1 °C/min to obtain TiO_2 powder samples. These powder samples were named according to the TNB : water molar ratios of 1 : 2, 1 : 4, 1 : 6 and the calcined temperature at 500 °C, 550 °C followed by P1:2-500, P1:4-500, P1:4-550, and P1:6-500.

2.2.2 Fabrication of nano TiO_2/monoliths

Fabrication of monolithic TiO_2 by a sol-gel dip-coating technique was performed with commercial honeycomb monoliths, SiO_2 and TiO_2 solutions. The commercial monoliths had been cleaned by an ultrasonic bath in acetone media for 30 min before being dried at 100 °C for 24 h to obtain cleaned monolith. The TiO_2 solutions in monolith fabrication and nanopowder synthesis were identical. The SiO_2 solution was prepared by adding dropwise an EtOH/H_2O solution with EtOH : H_2O molar ratio of 1 : 1 to a EtOH/TEOS solution with EtOH : TEOS molar ratio of 1 : 2. This mixture was adjusted pH value to 3 by using HNO_3 before stirred constantly for

12 h. PEG was added to the mixture with PEG : SiO_2 weight ratio of 1 : 2 afterwards. Stirring the mixture lasted another 6 h to acquire SiO_2 solution.
Monolithic TiO_2 samples were prepared by repeating a following dip-coating cycle. This cycle consisted of steps as follows. To begin dip-coating, the cleaned monoliths were immersed in the SiO_2 solution at a constant rate of 0.5 mm / s, then they were soaked in SiO_2 solution for 30 min and withdrawn at the same rate of immersion. The first cycle of SiO_2 coating was dried at 180 °C for 1 h before the monoliths were dip-coated with the SiO_2 solution one more time. The second cycle of SiO_2 coating was dried at 180 °C for 1 h before the monoliths were calcined at 600 °C or 800 °C for 3 h with a heating rate of 1 °C / min to obtain SiO_2 coated monolithic samples named SiO_2/M600 or SiO_2/M800. The SiO_2/M600 and SiO_2/M800 were performed sequentially dip-coating cycles into the SiO_2 solution two more times and into the TiO_2 solution two more times with the same speed as the previous SiO_2 coating cycles. The monolithic samples were dried at 180 °C after each cycle of SiO_2 coating and were dried at 120 °C after each cycle of TiO_2 coating. The TiO_2 coated monolithic samples were calcined at 500 °C for 2 h with a heating rate of 1 °C/min to complete the fabrication of monolithic samples named TiO_2/SiO_2/M600 and TiO_2/SiO_2/M800.

2.3 Characterization

Crystal phase of powder samples was determined by XRD using a D2 Phaser (Bruker) with Cu-Kα radiation (λ=0.15418 nm) at 0.02° step size and 0.2 s step time from 20° to 80°. Crystalline size was calculated by the Scherrer's equation (Eq(1)) at (101) peak, where β is the full width at half-maximum of the diffraction peak (FWHM, radian), k = 0.9 is a shape constant, D is the crystalline size and θ is the Bragg angle.

$$D = \frac{k.\lambda}{\beta.cos\varphi} \quad (1)$$

2.4 Antibacterial activity tests

A bacterial strain used in antibacterial tests was *Escherichia coli K12.* The bacterial culture in Luria-Bertani (LB) Broth was shaken with a shaking rate of 150 rpm at 30 °C for 18 h. The culture was centrifuged at 10,000 × g at 4 °C for 5 min to obtain a pellet. The pellet was suspended in the same volume of sterilized NaCl 0.8 % solution. The centrifugation and suspension were repeated to discard all residual LB Broth. The final pellet was suspended and serially diluted in sterilized NaCl 0.8 % solution to obtain a bacterial concentration of ~10^6 CFU mL^{-1}. The bacteria suspension containing ~10^6 CFU mL^{-1} was used in antibacterial activity tests for both the powder samples and the monolithic samples.

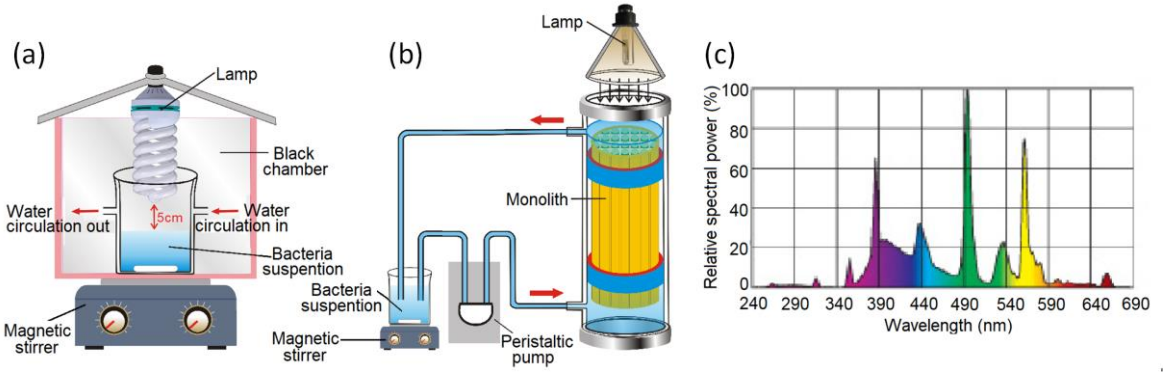

Figure 1: Illustration of photo-reactor used in the antibacterial activity test of (a) powder and (b) monolith samples and (c) the simulated solar light spectra of the lamp in the photo-reactor

In the case of the powder samples, the antibacterial activity test was performed in a photo-reactor illustrated in Figure 1a with a lamp as a simulated solar light source. The powder sample was added to the bacteria suspension to obtain a concentration of 1,000 ppm. Distance from the lamp to the suspension surface is 5 cm. The bacteria suspension was stirred constantly and its temperature was maintained at 30 ± 2 °C. A photolytic antibacterial test with simulated solar irradiation but without TiO_2 was performed to evaluate effect of the light source on bacteria.
In the case of the monolith samples, the antibacterial activity test was performed in a photo-reactor which contains a monolith and a simulated solar lamp (Figure 1b). The bacteria suspension was pumped circularly into the reactor at a flow rate of 70 mL / min by a peristaltic pump. The bacteria suspension was stirred

constantly and its temperature was maintained at 30 ± 2 °C. A “control” sample containing only bacteria suspension without TiO_2 and irradiation was always conducted simultaneously for each test in antibacterial activity of TiO_2. Conditions of the control test were the same as those of samples with presence of TiO_2. In all cases, the irradiation was maintained for 3 h and samples were taken every 30 min. They were serially diluted with 10, 100 or 1000-fold dilution and spread onto LB Agar plates. Bacteria concentration was estimated based on the number of colonies in the plates and the respective dilution levels.

3. Result and Discussion

Powder X-ray diffraction patterns of the powder samples are shown in Figure 2. It can be seen that all peaks of the powder samples calcined at 500 °C at 2θ diffraction angles of 25.2° (101), 36.9° (004), 48.24° (200), 54.86° (211) and 63.01° (204) are well-indexed with the JCPDS card No 21-1272. No diffraction peaks representing rutile phase as well as an impurity are detected in any samples calcined at 500 °C. It revealed that all of the samples including P1:2-500, P1:4-500 and P1:6-500 are pure anatase structures. According to the XRD results, crystalline size of the samples was calculated and displayed in Table 1. Among samples calcined at 500 °C, the crystalline size increased significantly from 13.2 nm to 18.4 nm according to decreasing of the TNB : water molar ratio. The TNB : H_2O molar ratio of 1 : 2 corresponding to the low amount of water not only causes a low rate of both hydrolysis and gelation (Bessekhouad et al., 2003) but also leads to producing small crystalline size. Because of lack of water, the probability of condensation progress in the oxolation manner is higher than the deoxolation one. Increasing the amount of water which supports formation of anatase structures also increases the hydrolysis rate. As a result, excess water promotes the deoxolation to create a large quantity of Ti–OH. They make primary particles be loosely packed lead to incomplete development of three-dimensional polymeric bonds (Bessekhouad et al., 2003). This explains the decrease of crystallization according to the rise of TNB : H_2O molar ratio from 1 : 4 to 1 : 6.

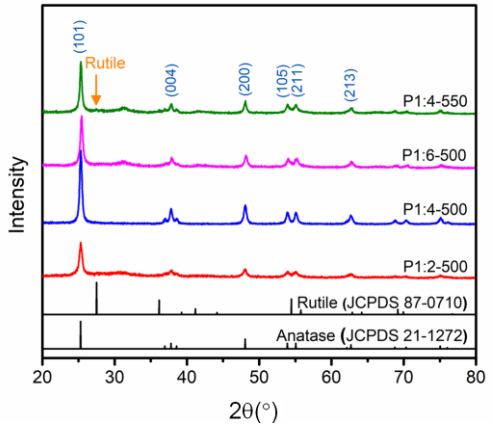

Figure 2: XRD patterns of powder TiO_2 samples: P1:2-500, P1:4-500, P1:6-500, and P1:4-550

Table 1: Crystalline size of powder samples

Sample	P1:2-500	P1:4-500	P1:6-500	P1:4-550
Average crystalline size (nm)	13.2	18.4	16.2	19.0

The P1:4-550 sample also indicated the peak at 2θ diffraction angles which are well-indexed with the JCPDS card No 21-1272. It disclosed that the anatase structure is still preserved according to the increment of calcined temperature from 500 °C to 550 °C. A less intense peak of rutile structure at a diffraction angle of 27.49° seen in the XRD result of P1:4-550 signed a transformation from anatase to rutile of TiO_2 which reduces crystallization of the anatase structure. Increasing the calcined temperature is accompanied by an increase of crystalline size clearly (Allen et al., 2018). This revealed that the calcined temperature is also an important factor which affects the crystal structure of TiO_2.

Antibacterial efficiency of the powder samples was displayed in Figure 3a. In the photolytic antibacterial with the lamp but without TiO_2 nanopowders, bacterial concentration was slightly decreased during 3 h, indicating simulated solar light source had almost no effect on the bacteria. In contrast, the bacterial concentration dramatically decreased by at least 3 log CFU mL^{-1} of *E. coli* after 3 h due to the presence of the TiO_2 nanopowder under irradiation. The ascending order of antibacterial activity is P1:6-500, P1:4-550, P1:2-500, P1:4-500, especially, P1:2-500 and P1:4-500. P1:4-500 demonstrated the highest antibacterial activity with a

3.2 log CFU mL^{-1} decrease of *E. coli* after only 1 h irradiation. In general, antibacterial activities depend on the crystallization of the anatase structure. The higher the crystallization of the anatase structure is, the higher the antibacterial activity of TiO_2 nanomaterial is. In contrast to this trend, the P1:2-500 sample is an exception. In spite of lower crystallization, its antibacterial activity was still higher than that of P1:6-500 or P1:4-550 sample. This result was probably caused by much smaller crystalline size, which increases the contact between TiO_2 nanoparticles and bacteria. Hence, crystalline size is also an important factor influencing the antibacterial activity of TiO_2 nanoparticles. The TiO_2 nanopowder sample synthesized with TNB : H_2O molar ratio of 1 : 4 and calcined temperature at 500 °C (P1:4-500) showed the highest antibacterial activity.

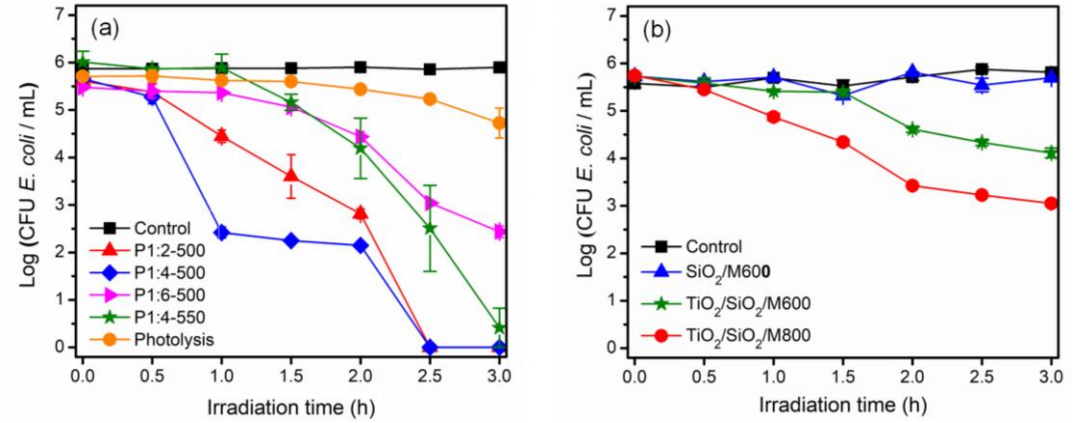

Figure 3: Antibacterial activity of (a) powder samples and (b) TiO_2-coated monolith samples according to irradiation time

The conditions to prepare the P1:4-500 sample were applied to the TiO_2 solution preparation that used for monolith coating. Optical fibers which support light transmission from the lamp to the narrow channels inside of monoliths are always required in monolithic photo-reactors to activate monolithic photocatalysts (Yu et al., 2011). Figure 3b described antibacterial activity of monolithic samples as a function of irradiation time. No antibacterial activity was shown in the SiO_2/M600 sample (without TiO_2). After 3 h irradiation, a 1.6 log CFU mL^{-1} decrease of *E. coli* at the TiO_2/SiO_2/M600 was shown, while the greater decrease of 2.7 log CFU mL^{-1} of *E. coli* was shown at the TiO_2/SiO_2/M800. It demonstrated that the nanoparticles were coated successfully on the channel monolith surface. The difference in the antibacterial activity of TiO_2/SiO_2/M600 and TiO_2/SiO_2/M800 was caused by SiO_2 background layer with various calcined temperature. SiO_2 in the background layer leads to improving smoothness of the inner monolithic surface and increases adhesion of the following TiO_2 layers. The higher calcined temperature (800 °C) caused the more adhesion between SiO_2 material and the monolith surface. It results in mechanical strengthen between TiO_2, SiO_2, and monolith that lead to elevate the photocatalytic activity of the sample.

4. Conclusions

The TiO_2 crystal structure was controlled by molar ratio of TNB: H_2O and calcined temperature. The TiO_2 nanoparticles were synthesized in single anatase phase. It was coated successfully on surface of monolith substrate by sol-gel method combined with dip-coating technique and using SiO_2 as a background layer which elevates adhesion of TiO_2. TiO_2/SiO_2/M800 sample reduced by 2.7 log CFU mL^{-1} of *E. coli* while TiO_2/SiO_2/M600 sample shown a 1.6 log CFU mL^{-1} decrease of *E. coli* after 3 h simulated solar irradiation. This study revealed that TiO_2/SiO_2/monolith is a potential photocatalyst in drinking water treatment under sunlight irradiation. The antibacterial activity of this material needs further enhancing in future studies.

Acknowledgments

This research is funded by Ho Chi Minh City University of Technology, VNU-HCM, under grant number BK-SDH-2020-1770444.

References

Allen N.S., Mahdjoub N., Vishnyakov V., Kelly P.J., Kriek R.J., 2018, The effect of crystalline phase (anatase, brookite and rutile) and size on the photocatalytic activity of calcined polymorphic titanium dioxide (TiO2), Polymer Degradation and Stability, 150, 31–36.

Baldursson S., Karanis P., 2011, Waterborne transmission of protozoan parasites: Review of worldwide outbreaks – An update 2004–2010, Water Research, 45(20), 6603-6614.
Bessekhouad Y., Robert D., Weber J.V., 2003, Synthesis of photocatalytic TiO2 nanoparticles: optimization of the preparation conditions, Journal of Photochemistry and Photobiology A: Chemistry, 157(1), 47–53.
Cao B., Cao S., Dong P., Gao J., Wang J., 2013, High antibacterial activity of ultrafine TiO2/graphene sheets nanocomposites under visible light irradiation, Materials Letters, 93, 349–352.
Feng C., Suzuki K., Zhao S., Sugiura N., Shimada S., Maekawa T., 2004, Water disinfection by electrochemical treatment, Bioresource Technology, 94(1), 21–25.
Galkina O.L., Sycheva A., Blagodatskiy A., Kaptay G., Katanaev V.L., Seisenbaeva G.A., Kessler V.G., Agafonov A.V., 2014, The sol–gel synthesis of cotton/TiO2 composites and their antibacterial properties, Surface and Coatings Technology, 253, 171–179.
Gaya U.I., Abdullah A.H., 2008, Heterogeneous photocatalytic degradation of organic contaminants over titanium dioxide: A review of fundamentals, progress and problems, Journal of Photochemistry and Photobiology C: Photochemistry Review, 9(1), 1–12.
Gumy D., Morais C., Bowen P., Pulgarin C., Giraldo S., Hajdu R., Kiwi J., 2006, Catalytic activity of commercial of TiO2 powders for the abatement of the bacteria (E. coli) under solar simulated light: Influence of the isoelectric point, Applied Catalysis B: Environmental, 63(1–2), 76–84.
Hakki H.K., Allahyari S., Rahemi N., Tasbihi M., 2018, The role of thermal annealing in controlling morphology, crystal structure and adherence of dip coated TiO2 film on glass and its photocatalytic activity, Materials Science in Semiconductor Processing, 85, 24–32.
Heck R.M., Gulati S., Farrauto R.J., 2001, The application of monoliths for gas phase catalytic reactions, Chemical Engineering Journal, 82(1–3), 149–156.
Hrudey S.E., 2009, Chlorination disinfection by-products, public health risk tradeoffs and me, Water Research, 43(8), 2057–2092.
Ismail A.F., Khulbe K.C., Matsuura T., 2019, RO Applications, Chapter In: Ismail A.F., Khulbe K. C., Matsuura T. (Eds.), Reverse osmosis, Elsevier, 221–248.
Laxma Reddy P.V., Kavitha B., Kumar Reddy P.A., Kim K.-H., 2017, TiO2-based photocatalytic disinfection of microbes in aqueous media: A review, Environmental Research, 154, 296–303.
Lee S.-Y., Park S.-J., 2013, TiO2 photocatalyst for water treatment applications, Journal of Industrial and Engineering Chemistry, 19(6), 1761–1769.
Liu X., Bae J., 2018, Urbanization and industrialization impact of CO2 emissions in China, Journal of Cleaner Production, 172, 178–186.
Lui G.Y., Roser D., Corkish R., Ashbolt N.J., Stuetz R., 2016, Point-of-use water disinfection using ultraviolet and visible light-emitting diodes, Science of The Total Environment, 553, 626–635.
Makhdoomi H., Moghadam H.M., Zabihi O., 2015, Effect of different conditions on the size and quality of titanium dioxide nanoparticles synthesized by a reflux process, Research on Chemical Intermediates, 41(3), 1777–1788.
Moongraksathum B., Chen Y.W., 2018, Anatase TiO2 co-doped with silver and ceria for antibacterial application, Catalysis Today, 310, 68–74.
Nguyen D.T., Ho T.N.S., Le M.V., 2019, Removal of ß-naphthol in water via photocatalytic degradation over N-TiO2/SiO2 nanocomposite under simulated solar light irradiation, Chemical Engineering Transactions, 72, 1–6.
Pichel N., Vivar M., Fuentes M., 2019, The problem of drinking water access: A review of disinfection technologies with an emphasis on solar treatment methods, Chemosphere, 218, 1014–1030.
Sasani Ghamsari M., Bahramian A.R., 2008, High transparent sol–gel derived nanostructured TiO2 thin film, Materials Letters, 62(3), 361–364.
Tahir M., 2018, Photocatalytic carbon dioxide reduction to fuels in continuous flow monolith photoreactor using montmorillonite dispersed Fe/TiO2 nanocatalyst, Journal of Cleaner Production, 170, 242-250.
Yang X., Peng J., Chen B., Guo W., Liang Y., Liu W., Liu L., 2012, Effects of ozone and ozone/peroxide pretreatments on disinfection byproduct formation during subsequent chlorination and chloramination, Journal of Hazardous Materials, 239-240, 348–354.
Yu Y.H., Pan Y.T., Wu Y.T., Lasek J., Wu J.C.S., 2011, Photocatalytic NO reduction with C3H8 using a monolith photoreactor, Catalysis Today, 174(1), 141–147.
Zeliger H.I., 2011, Water Pollution, Chapter In: Zeliger H.I. (Ed.), Human toxicology of chemical mixtures, 2nd Ed, William Andrew Publishing, Oxford, UK, 65–95.